Single and pair J/ψ production in the improved color evaporation model using the parton Reggeization approach

A. A. Chernyshev[*]
Samara National Research University, Samara 443086, Russia

V. A. Saleev[†]
Samara National Research University, Samara 443086, Russia and Joint Institute for Nuclear Research, Dubna 141980, Russia

(Received 17 November 2022; accepted 21 November 2022; published 8 December 2022)

In the article, we study single and pair J/ψ hadroproduction in the improved color evaporation model via the parton Reggeization approach. The last one is based on the k_T factorization of hard processes in multi-Regge kinematics, the Kimber-Martin-Ryskin-Watt model for unintegrated parton distribution functions, and the effective field theory of Reggezied gluons and quarks, suggested by L.N. Lipatov. We compare contributions from the single and double parton scattering mechanisms in the pair J/ψ production. The numerical calculations are realized using the Monte-Carlo event generator KaTie.

DOI: 10.1103/PhysRevD.106.114006

I. INTRODUCTION

Hadroproduction of J/ψ mesons has been intensively studied, theoretically and experimentally, for more than 50 years, after their discovery in 1974. Experimental data on single J/ψ production are obtained in a wide range of the energy from $\sqrt{s} = 19$ GeV up to $\sqrt{s} = 13$ TeV [1–9]. The processes of the pair production of J/ψ mesons were studied in experiments at the Large Hadron Collider (LHC) by the CMS [10], ATLAS [11], and LHCb [12] Collaborations at energies of 7, 8, and 13 TeV. The theoretical description of the processes of charmonium production is based on the perturbation theory of quantum chromodynamics (QCD) in the constant of strong interaction $\alpha_S(\mu)$, where the hard scale $\mu \sim m_\psi$, m_ψ is the charmonium mass and $\alpha_S \simeq 0.2$. The hadronization process of the $c\bar{c}$ pair to the charmonium is also described in terms of perturbation theory, only by the relative velocity of $c(\bar{c})$ quarks in the charmonium. It is implemented in the nonrelativistic quantum chromodynamics (NRQCD) approach [13]. In the leading approximation of the NRQCD, a quark and an antiquark are produced in the color singlet state, as assumed in the color singlet model (CSM) [14,15]. Despite the success of NRQCD in describing the charmonium spectra and cross sections at high energies, there are still unsolved problems: a description of η_c-meson production with allowance for the octet contribution of NRQCD leads to an excess of predictions over experimental data [16]; NRQCD predicts that prompt J/ψ should be produced mostly transversely polarized, however, experimentally this is not observed [17]. The latter ones may indicate the essential role of such nonperturbative effects that are not taken into account in the NRQCD. An alternative, but a more phenomenological approach, is the color evaporation model (CEM) proposed many years ago in Refs. [18,19]. Later, the CEM was improved by Ma and Vogt [20] and now is used to describe the spectra and polarizations of J/ψ mesons in the collinear parton model (CPM) [21,22] and in the k_T-factorization approach [23,24].

In the present study, we calculate the transverse momentum spectra of prompt J/ψ within the framework of the high energy factorization (HEF) or the k_T factorization, which initially has been introduced as a resummation tool for $\ln(\sqrt{s}/\mu)$-enhanced corrections to the hard-scattering coefficients in the CPM, where invariant $\sqrt{s}$ refers to the total energy of the process [25–27]. We use the parton Reggeization approach (PRA) which is a version of HEF formalism, based on the modified multi-Regge kinematics approximation for QCD scattering amplitudes [28–30]. The PRA is accurate both in the collinear limit, which drives the transverse-momentum-dependent factorization [31] and in the high-energy (multi-Regge) limit, which is important for Balitsky-Fadin-Kuraev-Lipatov [32–35] resummation of $\ln(\sqrt{s}/\mu)$-enhanced effects. In the PRA, we have studied successfully heavy quarkonium production in the proton-(anti)proton collisions at the Tevatron and the LHC using the NRQCD approach; see Refs. [36–39].

[*]aachernyshoff@gmail.com
[†]saleev@samsu.ru

The paper has the following structure. In Sec. II, the relevant basics of the PRA formalism are outlined. The Improved Color Evaporation Model (ICEM) is shortly reviewed in Sec. III. In Sec. IV, we overview Monte-Carlo (MC) parton-level event generator KaTie [40] and the relation between calculations via the PRA and KaTie for tree-level amplitudes. In Sec. V, we describe the experimental data for the single prompt J/ψ production at the energy range from 19 GeV up to 13 TeV. In Sec. VI, we describe the experimental data for the pair prompt J/ψ production at the energy of the LHC collider. Our conclusions are summarized in Sec. VII.

II. PARTON REGGEIZATION APPROACH

The PRA is based on the factorization hypothesis of the HEF or k_T factorization justified in the leading logarithmic approximation of the QCD at high energies [25–27]. Dependent on transverse momentum, parton distribution functions (PDF) of Reggeized quarks and gluons are calculated in the model proposed earlier by Kimber, Martin, Ryskin, and Watt (KMRW) [41,42], but with sufficient modifications [30] that will be described below. Reggeized parton amplitudes are constructed according to the Feynman rules of the L. N. Lipatov Effective Field Theory (EFT) of Reggeized gluons and quarks [43,44]. A detailed description of the PRA can be found in Refs. [28–30], inclusion of corrections from the emission of additional partons to the leading PRA approximation was studied in Refs. [29,45], and the development of the PRA with loop corrections was considered in Refs. [46–48].

In the PRA, the cross section of the process $p + p \to J/\psi + X$ is related to the cross section of the parton subprocess by the factorization formula

$$d\sigma = \sum_{i,\bar{j}} \int_0^1 \frac{dx_1}{x_1} \int \frac{d^2\mathbf{q}_{T1}}{\pi} \Phi_i(x_1, t_1, \mu^2) \times \int_0^1 \frac{dx_2}{x_2} \int \frac{d^2\mathbf{q}_{T2}}{\pi} \Phi_j(x_2, t_2, \mu^2) \cdot d\hat{\sigma}_{\mathrm{PRA}}, \quad (1)$$

where $t_{1,2} = -\mathbf{q}^2_{T1,2}$, the cross section of the subprocess with Reggeized partons $\hat{\sigma}_{\mathrm{PRA}}$ is expressed in terms of squared Reggeized amplitudes $\overline{|\mathcal{A}_{\mathrm{PRA}}|^2}$ in the standard way.

The PRA hard-scattering amplitudes are gauge invariant because the initial-state off-shell partons are considered as Reggeized partons of the gauge-invariant EFT for QCD processes in the multi-Regge kinematics limit [43,44]. The Feynman rules of the Lipatov EFT are written down in Refs. [44,49]. The easy way to use Feynman rules of Lipatov EFT is to explore a model file ReggeQCD [29] for the FeynArts tool [50].

Unintegrated PDFs (unPDFs) in the modified KMRW model are calculated by the formula [30]

$$\Phi_i(x, t, \mu) = \frac{\alpha_s(\mu)}{2\pi} \frac{T_i(t, \mu^2, x)}{t} \sum_{j=q,\bar{q},g} \int_x^1 dz\, P_{ij}(z) F_j\left(\frac{x}{z}, t\right) \times \theta(\Delta(t, \mu) - z), \quad (2)$$

where $F_i(x, \mu_F^2) = x f_j(x, \mu_F^2)$. Here and below, factorization and renormalization scales are equal, $\mu_F = \mu_R = \mu$, and $\Delta(t, \mu^2) = \sqrt{t}/(\sqrt{\mu^2} + \sqrt{t})$ is the KMRW-cutoff function [41]. To resolve the collinear divergence problem, we require that the modified unPDF $\Phi_i(x, t, \mu)$ should be satisfied by the exact normalization condition:

$$\int_0^{\mu^2} dt \Phi_i(x, t, \mu^2) = F_i(x, \mu^2), \quad (3)$$

or

$$\Phi_i(x, t, \mu^2) = \frac{d}{dt}[T_i(t, \mu^2, x) F_i(x, t)], \quad (4)$$

where $T_i(t, \mu^2, x)$ is the Sudakov form factor, $T_i(t = 0, \mu^2, x) = 0$ and $T_i(t = \mu^2, \mu^2, x) = 1$. The explicit form of the Sudakov form factor in (4) was first obtained in [30]:

$$T_i(t, \mu^2, x) = \exp\left[-\int_t^{\mu^2} \frac{dt'}{t'} \frac{\alpha_s(t')}{2\pi} (\tau_i(t', \mu^2) + \Delta\tau_i(t', \mu^2, x))\right], \quad (5)$$

where

$$\tau_i(t, \mu^2) = \sum_j \int_0^1 dz\, z P_{ji}(z) \theta(\Delta(t, \mu^2) - z),$$

$$\Delta\tau_i(t, \mu^2, x) = \sum_j \int_0^1 dz\, \theta(z - \Delta(t, \mu^2)) \times \left[z P_{ji}(z) - \frac{F_j(\frac{x}{z}, t)}{F_i(x, t)} P_{ij}(z) \theta(z - x)\right].$$

In contrast to the KMRW model, the Sudakov form factor (5) depends on x, which is necessary to preserve the exact normalization (3) for any x and μ. The gauge invariance of amplitudes with Reggeized partons in the PRA allows you to study any processes described by non-Abelian QCD structures. PRA has been successfully used for descriptions of angular correlations in two-jet events [28], production of the charm [51,52] and beauty mesons [29,53], and charmonium in the NRQCD [54,55].

III. IMPROVED COLOR EVAPORATION MODEL

The current status of the ICEM is presented in Ref. [20]. In the PRA, the initial partons have transverse momenta, so the description of the spectra of single J/ψ is already possible at the leading order approximation in the strong interaction constant in the parton subprocesses

$$R + R \to c + \bar{c} \tag{6}$$

and

$$Q_q + \bar{Q}_q \to c + \bar{c}, \tag{7}$$

where R is a Reggeized gluon, $Q_q(\bar{Q}_q)$ is a Reggeized quark (antiquark), and $q = u, d, s$.

In the ICEM, the cross section for the production of prompt J/ψ mesons is related to the cross section for the production of $c\bar{c}$ pairs in the single parton scattering (SPS) as follows:

$$\sigma^{\rm SPS}(p + p \to J/\psi + X) = \mathcal{F}^{\psi} \times \int_{m_\psi}^{2m_D} \frac{d\sigma(p + p \to c + \bar{c} + X)}{dM} dM, \tag{8}$$

where M is the invariant mass of the $c\bar{c}$ pair with 4-momentum $p^\mu_{c\bar{c}} = p^\mu_c + p^\mu_{\bar{c}}$, m_ψ is the mass of the J/ψ meson, and m_D is the mass of the lightest D meson. To take into account the kinematic effect associated with the difference between the masses of the intermediate state and the final charmonium, the 4-momentum of the $c\bar{c}$ pair and J/ψ meson are related by $p^\mu_\psi = (m_\psi/M)p^\mu_{c\bar{c}}$. The universal parameter $\mathcal{F}^\psi$ is considered as a probability of transformation of the $c\bar{c}$ pair with invariant mass $m_\psi < M < 2m_D$ into the prompt J/ψ meson.

In case of pair J/ψ production via the SPS, we take into account contributions of the following subprocesses:

$$R + R \to c + \bar{c} + c + \bar{c} \tag{9}$$

and

$$Q_q + \bar{Q}_q \to c + \bar{c} + c + \bar{c}. \tag{10}$$

The cross section for the production of a pair of prompt J/ψ mesons is related to the cross section for the production of two pairs of $c\bar{c}$ quarks in the following way:

$$\sigma^{\rm SPS}(p + p \to J/\psi + J/\psi + X) = \mathcal{F}^{\psi\psi} \times \int_{m_\psi}^{2m_D} \int_{m_\psi}^{2m_D} \frac{d\sigma(p + p \to c_1 + \bar{c}_1 + c_2 + \bar{c}_2 + X)}{dM_1 dM_2} dM_1 dM_2, \tag{11}$$

where $M_{1,2}$ are the invariant masses of $c\bar{c}$ pairs with 4-momenta $p^\mu_{c\bar{c}1} = p^\mu_{c1} + p^\mu_{\bar{c}1}$ and $p^\mu_{c\bar{c}2} = p^\mu_{c2} + p^\mu_{\bar{c}2}$. Parameter $\mathcal{F}^{\psi\psi}$ is the probability of transformation of two pairs $c\bar{c}$ with invariant masses $m_\psi < M_{1,2} < 2m_D$ into two J/ψ mesons.

In the double parton scattering (DPS) approach [56], the cross section for the production of a J/ψ pair is written in terms of the cross sections for the production of a single J/ψ in two independent subprocesses

$$\sigma^{\rm DPS}(p + p \to J/\psi + J/\psi + X) = \frac{\sigma^{\rm SPS}(p + p \to J/\psi + X_1) \times \sigma^{\rm SPS}(p + p \to J/\psi + X_2)}{2\sigma_{\rm eff}}, \tag{12}$$

where the parameter $\sigma_{\rm eff}$, which controls the contribution of the DPS mechanism is considered a free parameter. Thus, at fitting cross sections for pair J/ψ-meson production, we assume that the parameter $\mathcal{F}^\psi$ is fixed, and the parameters $\mathcal{F}^{\psi\psi}$ and $\sigma_{\rm eff}$ are free parameters.

IV. NUMERICAL METHODS

The full gauge-invariant set of Feynman diagrams of the Lipatov EFT for the subprocess (9) contains 72 diagrams. It is getting too large for analytical calculation. To proceed to the next step, we should analytically calculate squared off-shell amplitudes and perform a numerical integration using factorization formula (1) with the modified unPDFs (2). Nowadays, we can do it with the required numerical accuracy only for $2 \to 2$ (6,7) or $2 \to 3$ [29] off-shell parton subprocesses. To calculate contributions from $2 \to 4$ subprocesses with initial Reggeized partons we should apply fully numerical methods of the calculation.

A few years ago, a new approach to obtaining gauge invariant amplitudes with off-shell initial-state partons in scattering at high energies was proposed. The method is based on the use of spinor amplitude formalism and recurrence relations of the Britto-Cachazo-Feng-Witten type [57,58]. In Ref. [40] the MC parton-level event generator KaTie for processes at high energies with nonzero transverse

TABLE I. The parameter $\mathcal{F}^{\psi}$ at the kinematical conditions of the different experiments.

Collaboration	Energy	Rapidity	Transverse Momentum	$\mathcal{F}^{\psi}$
NA3:	$\sqrt{s} = 19.4$ GeV	$y > 0$	$p_T \in [0, 5]$ GeV	$0.213^{+0.008}_{-0.008}$
AFS:	$\sqrt{s} = 30$ GeV	$\lvert y\rvert < 0.5$	$p_T \in [0, 5]$ GeV	$0.201^{+0.026}_{-0.026}$
	$\sqrt{s} = 53$ GeV	$\lvert y\rvert < 0.5$	$p_T \in [0, 7]$ GeV	$0.121^{+0.012}_{-0.012}$
PHENIX:	$\sqrt{s} = 200$ GeV	$\lvert y\rvert < 0.35$	$p_T \in [0, 9]$ GeV	$0.102^{+0.033}_{-0.033}$
CDF:	$\sqrt{s} = 1.96$ TeV	$\lvert y\rvert < 0.6$	$p_T \in [0, 20]$ GeV	$0.044^{+0.018}_{-0.018}$
LHCb:	$\sqrt{s} = 5$ TeV	$2.0 < y < 2.5$	$p_T \in [0, 14]$ GeV	$0.025^{+0.007}_{-0.007}$
ALICE:	$\sqrt{s} = 7$ TeV	$\lvert y\rvert < 0.9$	$p_T \in [0, 7]$ GeV	$0.037^{+0.007}_{-0.007}$
ATLAS:	$\sqrt{s} = 7$ TeV	$\lvert y\rvert < 0.75$	$p_T \in [7, 70]$ GeV	$0.013^{+0.002}_{-0.001}$
		$0.75 < \lvert y\rvert < 1.50$	$p_T \in [5, 70]$ GeV	$0.007^{+0.001}_{-0.001}$
		$1.5 < \lvert y\rvert < 2.0$	$p_T \in [1, 30]$ GeV	$0.011^{+0.001}_{-0.001}$
		$2.0 < \lvert y\rvert < 2.4$	$p_T \in [5, 30]$ GeV	$0.009^{+0.001}_{-0.001}$
CMS:	$\sqrt{s} = 7$ TeV	$\lvert y\rvert < 0.9$	$p_T \in [8, 70]$ GeV	$0.005^{+0.001}_{-0.001}$
		$0.9 < \lvert y\rvert < 1.2$	$p_T \in [8, 45]$ GeV	$0.007^{+0.001}_{-0.002}$
		$1.2 < \lvert y\rvert < 1.6$	$p_T \in [6.5, 45]$ GeV	$0.007^{+0.002}_{-0.002}$
		$1.6 < \lvert y\rvert < 2.1$	$p_T \in [6.5, 30]$ GeV	$0.009^{+0.002}_{-0.002}$
		$2.1 < \lvert y\rvert < 2.4$	$p_T \in [5.5, 30]$ GeV	$0.009^{+0.002}_{-0.002}$
LHCb:	$\sqrt{s} = 13$ TeV	$2.0 < y < 2.5$	$p_T \in [0, 14]$ GeV	$0.021^{+0.004}_{-0.004}$
		$2.5 < y < 3.0$	$p_T \in [0, 14]$ GeV	$0.022^{+0.004}_{-0.004}$
		$3.0 < y < 3.5$	$p_T \in [0, 14]$ GeV	$0.021^{+0.004}_{-0.004}$
		$3.5 < y < 4.0$	$p_T \in [0, 14]$ GeV	$0.018^{+0.005}_{-0.005}$

momenta and virtualities was developed. This formalism [57,58] for numerical amplitude generation is equivalent to amplitudes built according to Feynman rules of the Lipatov EFT at the level of tree diagrams [28,29,59]. At the stage of numerical calculations, we use the MC event generator KaTie [40] for calculating the proton-proton cross sections with contributions of all subprocesses (6), (7), (9), and (10). The accuracy of numerical calculations for total proton-proton cross sections is equal to 0.1%.

V. SINGLE J/ψ PRODUCTION

We have performed the fit procedure for prompt J/ψ transverse momenta spectra in the ICEM via the PRA with $\mathcal{F}^{\psi}$ as a free parameter and obtained a rather good agreement between the calculations and experimental data from the energy 19.4 GeV up to 13 TeV as it was measured by different collaborations [1–9]. The obtained results are collected in Table I and presented in Fig. 1. Thus, as $\sqrt{s}$

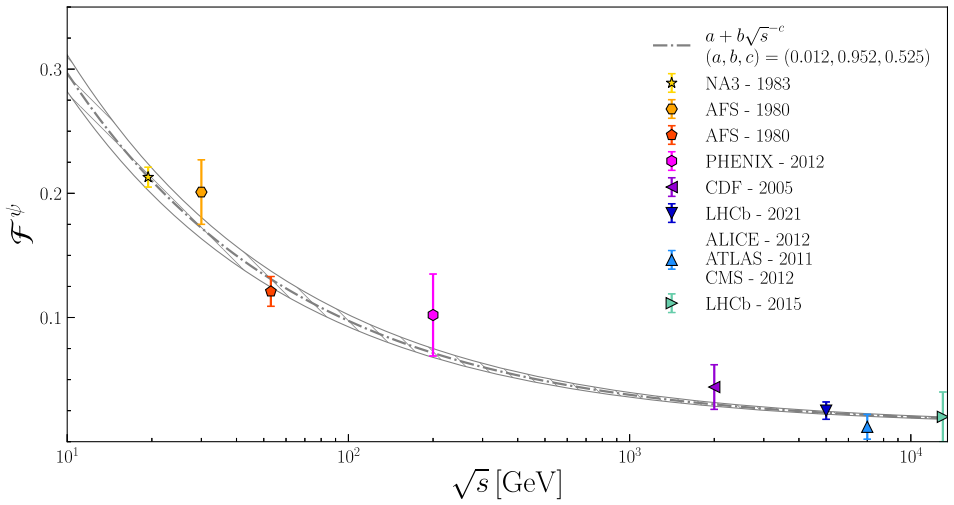

FIG. 1. The hadronization parameter $\mathcal{F}^{\psi}$ as a function of proton collision energy $\sqrt{s}$. The corridor between the upper and lower lines demonstrates the uncertainty from the hard scale variation by the factor $\xi = 2$ and the c-quark mass from 1.2 to 1.4 GeV.

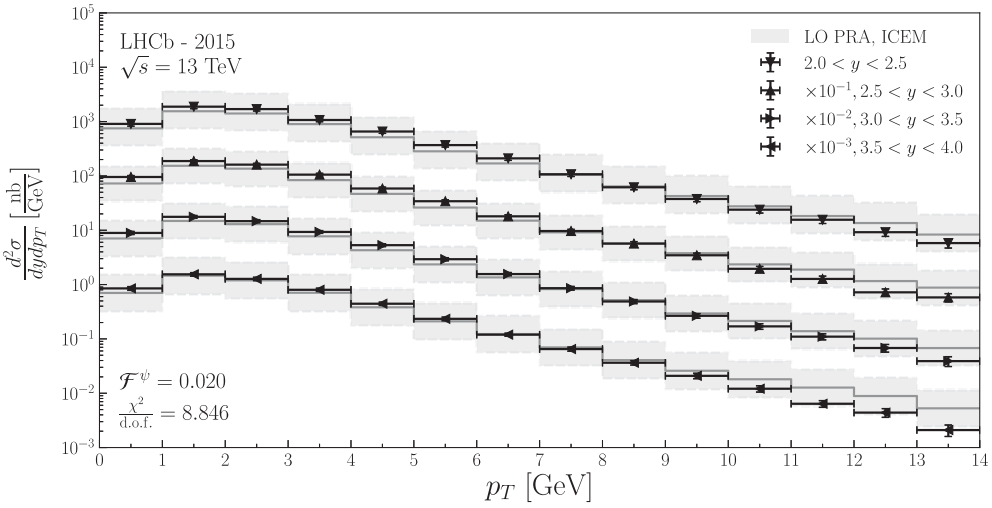

FIG. 2. The transverse momentum spectra of prompt J/ψ at the different ranges of rapidities. The data are from the LHCb Collaboration at the $\sqrt{s} = 13$ TeV [9].

decreases from 13 TeV to 19 GeV, the factor F^{ψ} increases by an order of magnitude, from about 0.02 up to 0.2. If we interpret the parameter $\mathcal{F}^{\psi}$ as the probability of transformation of the $c\bar{c}$ pair with invariant mass from m_{ψ} to $2m_D$ into the J/ψ meson, its growth with decreasing energy can be explained by an increase of the hadronization time. The energy dependence of the $\mathcal{F}^{\psi}$ is well described by a formula

$$\mathcal{F}^{\psi}(\sqrt{s}) = 0.012 + 0.952(\sqrt{s})^{-0.525}. \tag{13}$$

The calculated transverse momentum spectra and the experimental data are presented in Figs. 2–8. Grey boxes around the central lines in the figures indicate upper and lower limits of the cross section obtained due to the variation of the hard scale μ by the factors $\xi = 2$ or $\xi = 1/2$ around the central value of the hard scale ($\mu = \sqrt{m_{\psi}^2 + p_T^2}$) and the c-quark mass from 1.2 to 1.4 GeV.

In contrast to the predictions obtained in the NRQCD approach, when gluon-gluon fusion in the J/ψ hadroproduction is the dominant mechanism, the ICEM predicts a sufficiently large contribution from the process of quark-antiquark annihilation especially at low energy; see Fig. 9. Thus, at the energy of future proton-proton collider NICA, $\sqrt{s} \simeq 30$ GeV, the quark-antiquark contribution may be about 30% of the total cross section of prompt J/ψ production.

VI. PAIR J/ψ PRODUCTION

In Ref. [60], the pair J/ψ production was studied in the next to leading order approximation of the collinear parton model. The authors assumed

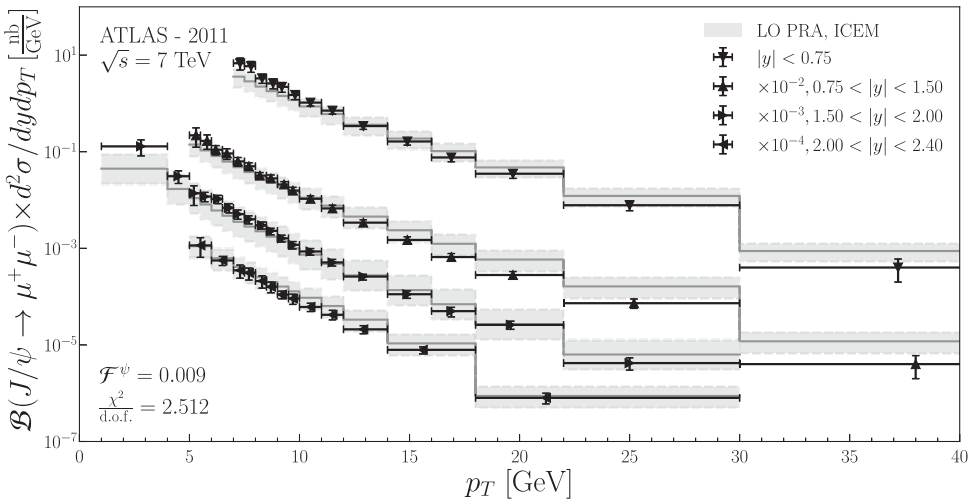

FIG. 3. The transverse momentum spectra of prompt J/ψ at the different ranges of rapidities. The data are from the ATLAS Collaboration at the $\sqrt{s} = 8$ TeV [7].

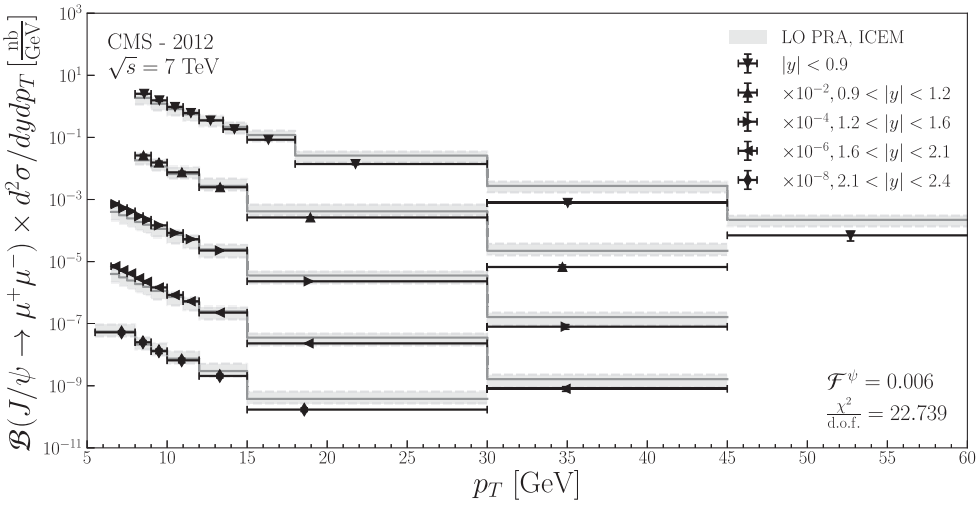

FIG. 4. The transverse momentum spectra of prompt J/ψ at the different ranges of rapidities. The data are from the CMS Collaboration at the $\sqrt{s} = 8$ TeV [8].

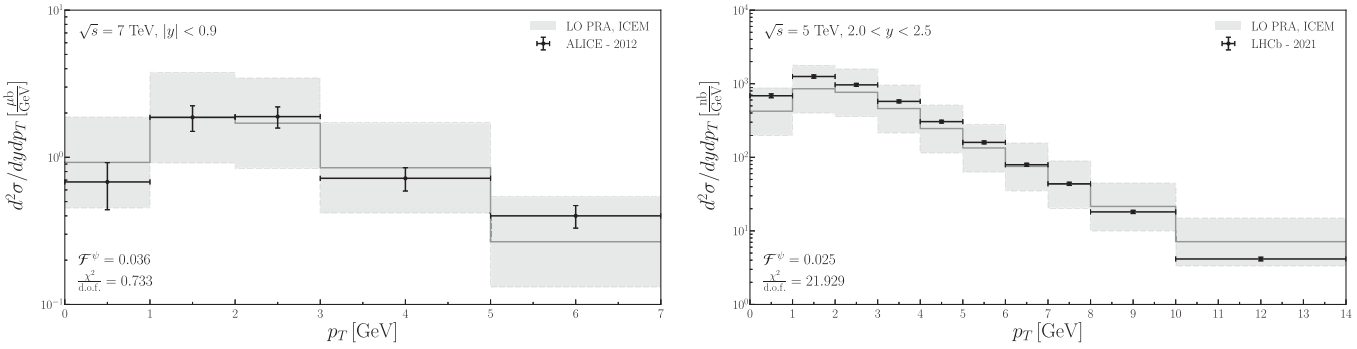

FIG. 5. The transverse momentum spectra of prompt J/ψ. In the left panel, the data are from the ALICE Collaboration at the $\sqrt{s} = 7$ TeV [6]. In the right panel, the data are from the LHCb Collaboration at the $\sqrt{s} = 5$ TeV [5].

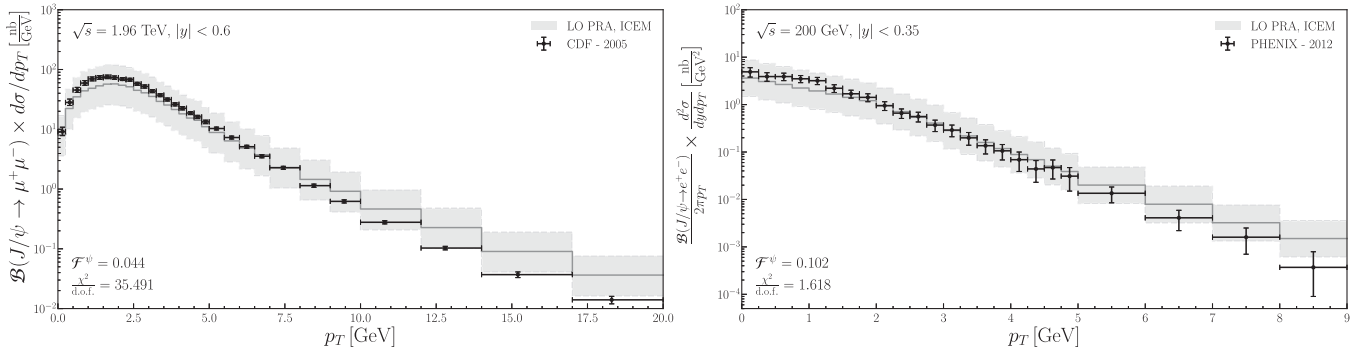

FIG. 6. The transverse momentum spectra of prompt J/ψ. In the left panel, the data are from the CDF Collaboration at the $\sqrt{s} = 1.8$ TeV [4]. In the right panel, the data are from the PHENIX Collaboration at the $\sqrt{s} = 0.2$ TeV [3].

$$\mathcal{F}^{\psi\psi} = (\mathcal{F}^{\psi})^2 \tag{14}$$

and found that the contribution of the SPS production mechanism is negligible and the experimental data can only be described by the DPS mechanism. In our opinion, the relation (14) is valid only in the case of the dominant role of the fragmentation approximation for the production of the J/ψ pair. However, the fragmentation mechanism of J/ψ

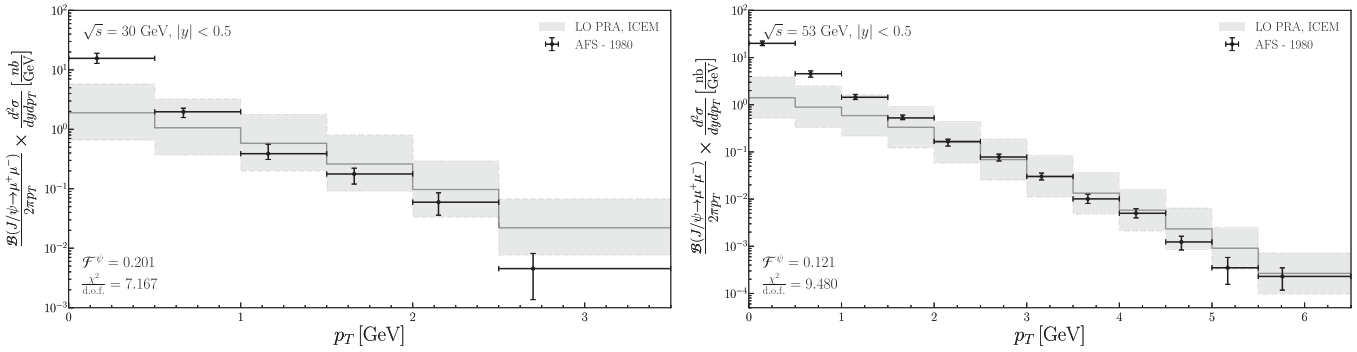

FIG. 7. The transverse momentum spectra of prompt J/ψ. In the left panel, the data are from the AFS Collaboration, at the $\sqrt{s} = 30$ GeV [2]. In the right panel, the data are from the AFS Collaboration at the $\sqrt{s} = 53$ GeV [2].

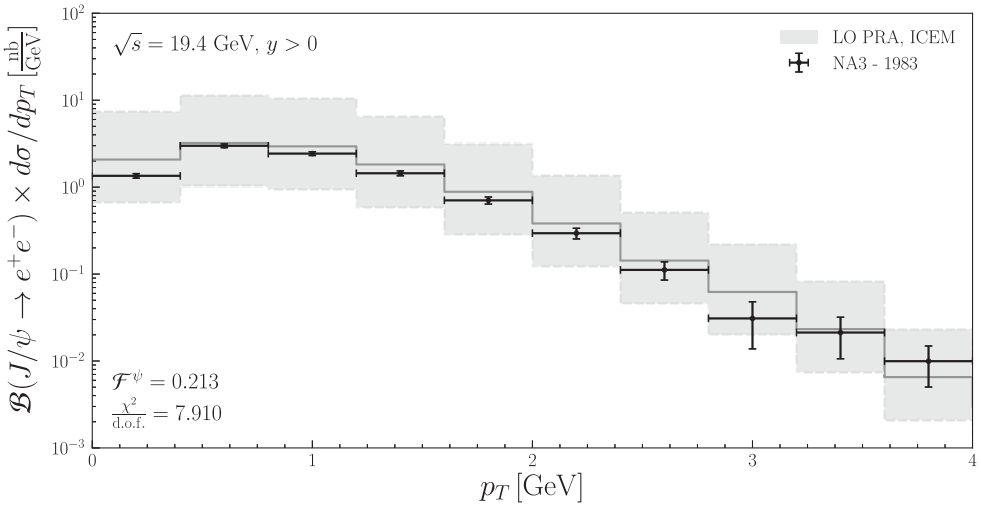

FIG. 8. The transverse momentum spectrum of prompt J/ψ. The data are from the NA3 Collaboration at the $\sqrt{s} = 19.4$ GeV [1].

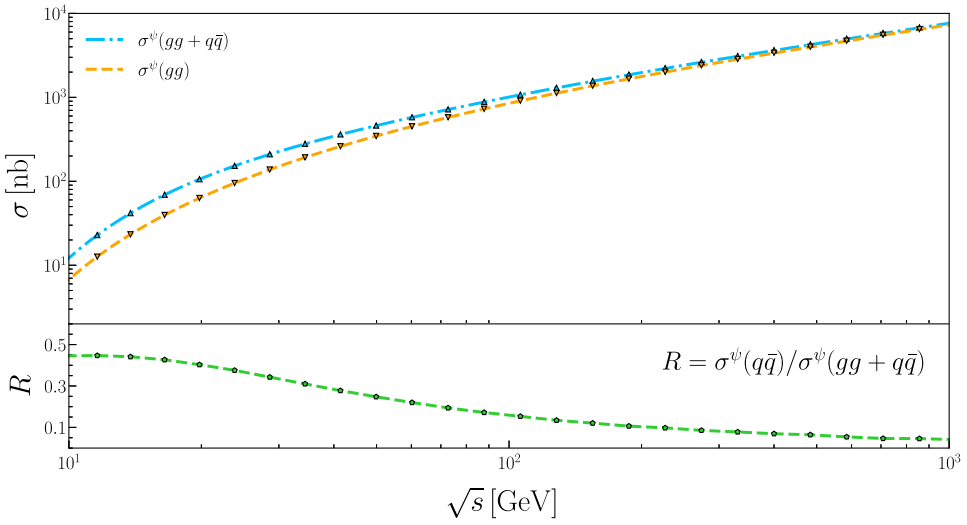

FIG. 9. The relative contributions of the parton subprocess (6) and (7) in the prompt J/ψ production as a function of energy obtained in the ICEM via the PRA.

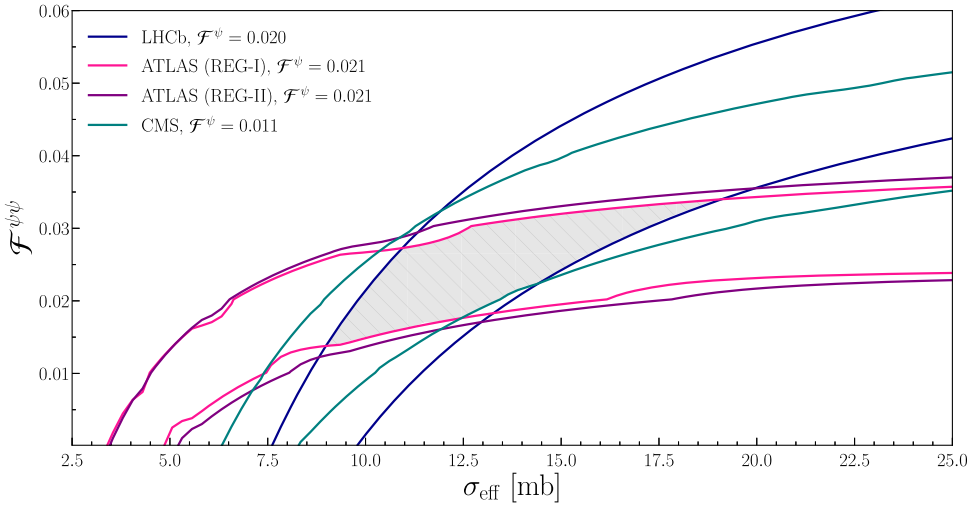

FIG. 10. Regions of the parameters $\mathcal{F}^{\psi\psi}$ and $\sigma_{\rm eff}$ in the ICEM for pair J/ψ production, obtained as a result of data fitting. The relevant pairs of isolines correspond to $x_k = \pm 1.0$ for different experiments.

production becomes dominant for $p_T^{\psi} \geq 15$ GeV, i.e., at much larger transverse momentum of the J/ψ than that at which the measurements [10–12] were made.

First of all, we review the setup of the pair J/ψ measurements:

(i) LHCb, $\sqrt{s} = 13\,\text{TeV}, 2.0 < y^{\psi} < 4.5, p_T^{\psi} < 10.0\,\text{GeV}$.
(ii) ATLAS (REG-I), $\sqrt{s} = 8$ TeV, $|y^{\psi_1}| < 2.10$, $p_T^{\psi_1} > 8.5$ GeV, $|y^{\psi_2}| < 1.05$, $p_T^{\psi_2} > 8.5$ GeV, where $p_T^{\psi_2} < p_T^{\psi_1}$.
(iii) ATLAS (REG-II), $\sqrt{s} = 8$ TeV, $|y^{\psi_1}| < 2.10$, $p_T^{\psi_1} > 8.5$ GeV, $1.05 < |y^{\psi_2}| < 2.10$, $p_T^{\psi_2} > 8.5\,\text{GeV}$, where $p_T^{\psi_2} < p_T^{\psi_1}$.
(iv) CMS (REG-I), $\sqrt{s} = 7$ TeV, $|y^{\psi}| < 1.20$, $p_T^{\psi} > 6.5$ GeV.
(v) CMS (REG-II), $\sqrt{s} = 7$ TeV, $1.20 < |y^{\psi}| < 1.43$, $p_T^{\psi} \in (6.5 \to 4.5)$ GeV.
(vi) CMS (REG-III), $\sqrt{s} = 7$ TeV, $1.43 < |y^{\psi}| < 2.20$, $p_T^{\psi} > 4.5$ GeV.

In the case of pair J/ψ production, we took into account the contributions of the SPS and the DPS production mechanisms. Parameters $\mathcal{F}^{\psi\psi}$ and $\sigma_{\rm eff}$ obtained by the separate fits of production cross sections for different experiments are shown as a contour plot in Fig. 10. Two curves for each experiment ($k = \text{LHCb, ATLAS, CMS}$) correspond to $x_k = \pm 1$, where

$$x_k = \frac{\sigma_k^{\rm exp} - \sigma_k^{\rm theor}}{\Delta\sigma_k^{\rm exp}}.$$

We find that there is a common region of parameters $\mathcal{F}^{\psi\psi}$ and $\sigma_{\rm eff}$ for all experiments. If we collect all experimental

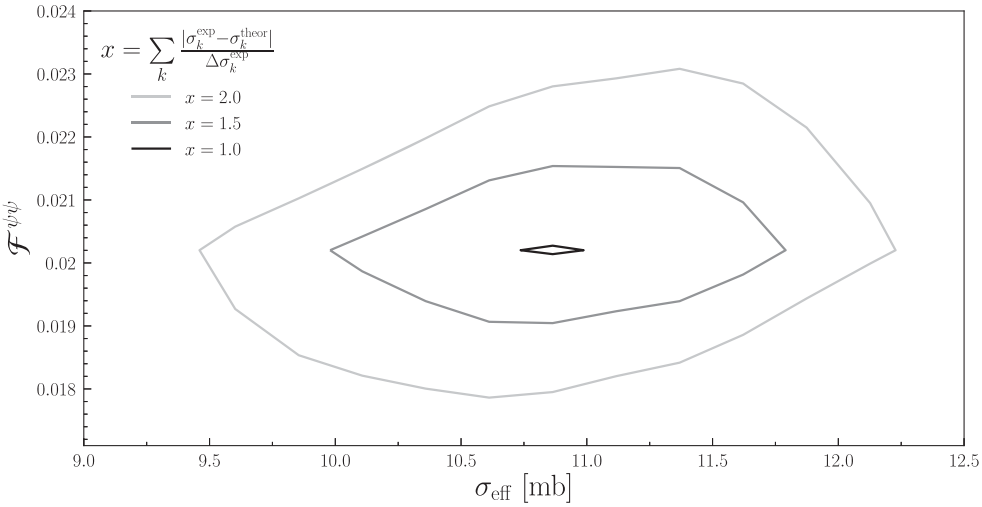

FIG. 11. Regions of the parameters $\mathcal{F}^{\psi\psi}$ and $\sigma_{\rm eff}$ in the ICEM for pair J/ψ production, obtained as a result of data fitting. Isolines correspond to $x = 1.0$, 1.5 and 2.0.

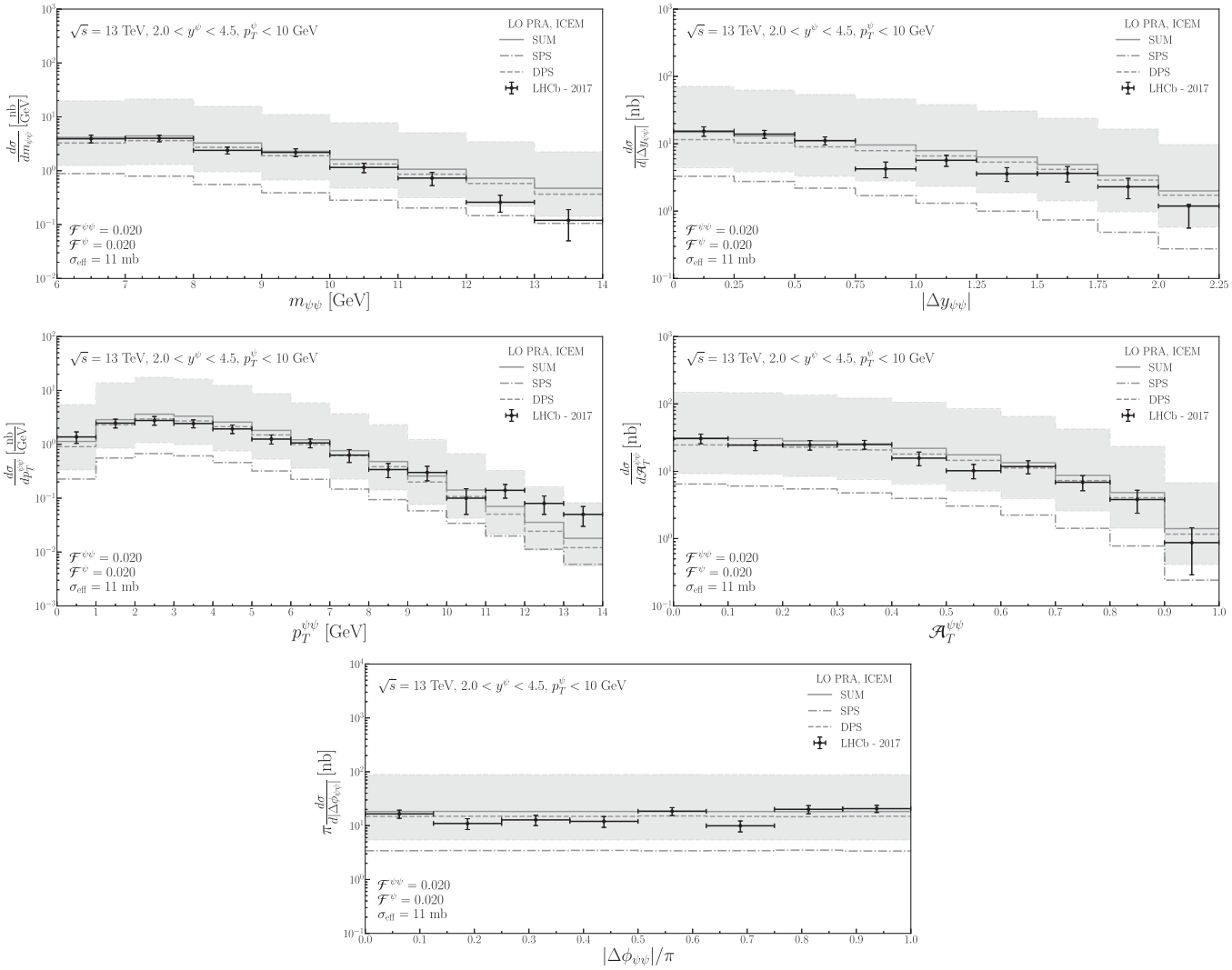

FIG. 12. Different spectra of pair J/ψ production on $m_{\psi\psi}$, $|\Delta y_{\psi\psi}|$, $p_T^{\psi\psi}$, $A_T^{\psi\psi}$, and $|\Delta\phi^{\psi\psi}|$. The data are from the LHCb Collaboration [12].

data into one set for the fit, we find more strong conditions in a plane of these two parameters, which are shown as a contour plot in Fig. 11. The isolines correspond to the numerical values of the parameter $x = 1.0$, 1.5, and 2.0, where

$$x = \sum_{k=1}^{n} \frac{|\sigma_k^{\rm exp} - \sigma_k^{\rm theor}|}{\Delta\sigma_k^{\rm exp}}$$

and the sum is taken over all cross sections of three experiments: CMS [10], ATLAS [11], and LHCb [12]. The best description of the data, when $x < 1.0$, is reached in the parameter domain $0.021 < \mathcal{F}^{\psi\psi} < 0.023$ and $10.75 < \sigma_{\rm eff} < 11.2$ mb. In fact, at the LHC energies one has $\mathcal{F}^{\psi\psi} \simeq \mathcal{F}^{\psi}$. The optimal obtained value for $\sigma_{\rm eff}$ is in a good agreement with the estimates obtained early in other studies [10,12].

To demonstrate agreement between our calculations in the ICEM via the PRA and experimental data for pair J/ψ production, we plot in Figs. 12–14 different spectra, which have been obtained with $\mathcal{F}^{\psi} = 0.02$, $\mathcal{F}^{\psi\psi} = 0.02$, and $\sigma_{\rm eff} = 11$ mb. It is interesting to compare the ratio of the SPS and DPS contributions, $R = \sigma_{\psi\psi}^{\rm SPS}/\sigma_{\psi\psi}^{\rm DPS}$, to the pair J/ψ production cross sections with the above mentioned values of $\mathcal{F}^{\psi}$, $\mathcal{F}^{\psi\psi}$, and $\sigma_{\rm eff}$: for the LHCb data ($\sqrt{s} = 13$ TeV)—$R \simeq 0.2$, for the CMS data ($\sqrt{s} = 7$ TeV)—$R \simeq 0.5$, but for the ATLAS data ($\sqrt{s} = 8$ TeV)—$R \simeq 1.5$. In such a way, the DPS production mechanism is a dominant source of J/ψ pairs only when both J/ψ are produced in the forward region of rapidity, as it is measured by LHCb Collaboration.

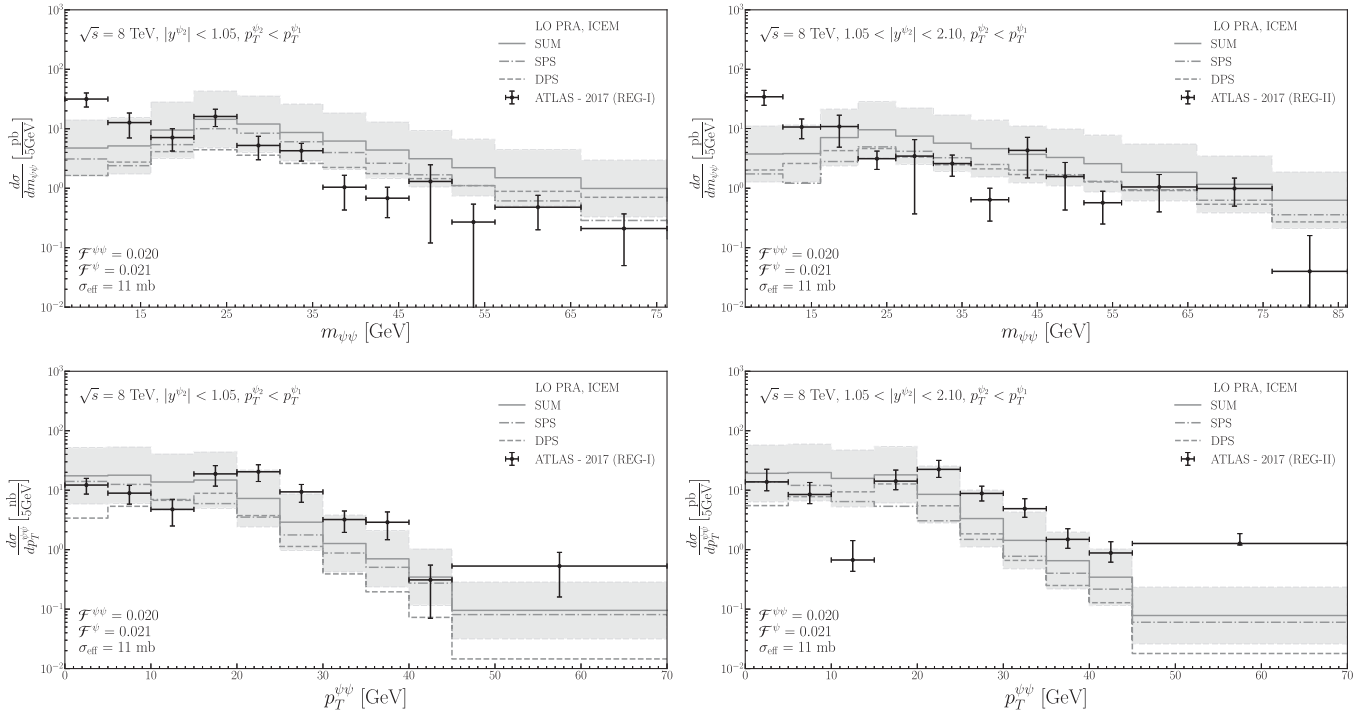

FIG. 13. Different spectra of pair J/ψ production on $m_{\psi\psi}$ and $p_T^{\psi\psi}$ for central and forward rapidity regions. The data are from the ATLAS Collaboration [11].

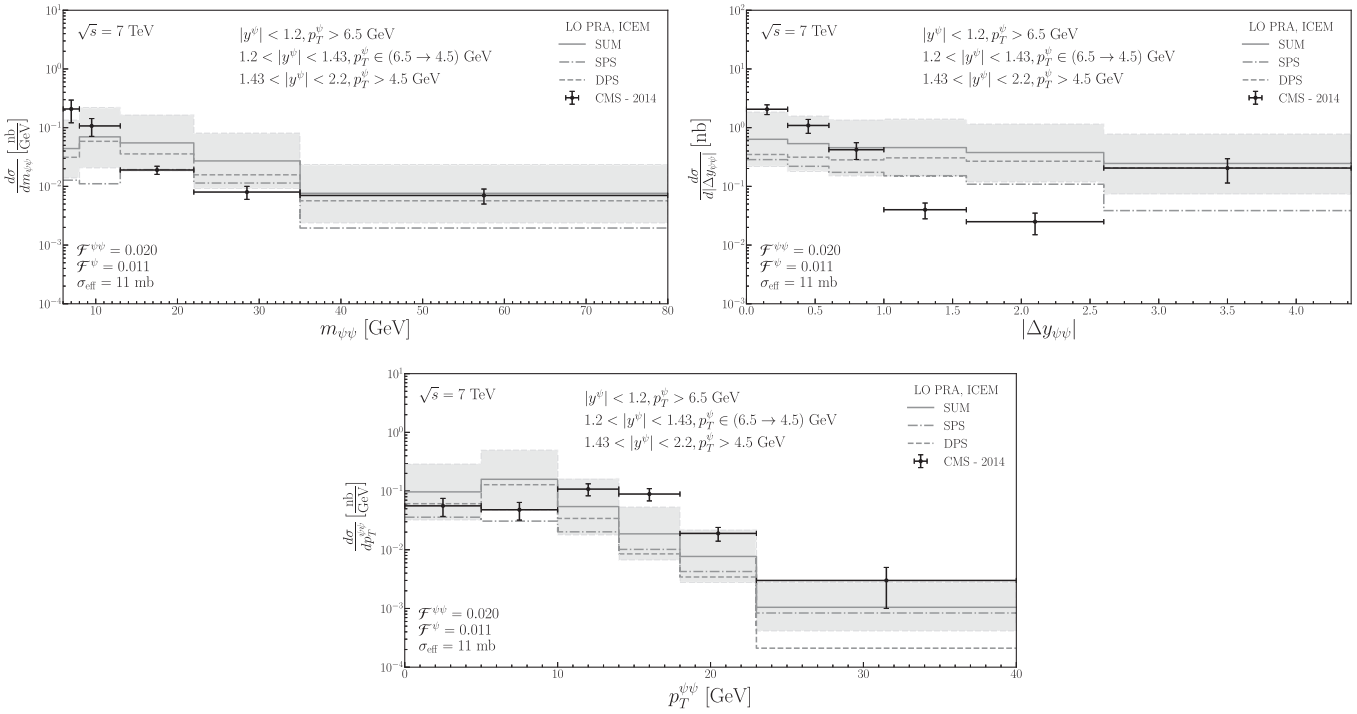

FIG. 14. Different spectra of pair J/ψ production on $m_{\psi\psi}$, $|\Delta\phi^{\psi\psi}|$, and $p_T^{\psi\psi}$. The data are from the CMS Collaboration [10].

VII. CONCLUSIONS

We obtain a quite satisfactory description for the single prompt J/ψ p_T spectra and cross sections in the ICEM using the PRA at the wide range of the collision energy. The obtained values of the hadronization parameter $\mathcal{F}^{\psi}$ depend on energy, and such dependence can be approximated by the formula $\mathcal{F}^{\psi}(\sqrt{s}) = 0.012 + 0.952(\sqrt{s})^{-0.525}$. The exact physical interpretation of such energy dependence needs special analysis.

Both mechanisms, SPS and DPS, for the pair J/ψ production have been considered. We show the assumption $\mathcal{F}^{\psi\psi} = \mathcal{F}^{\psi} \times \mathcal{F}^{\psi}$ is not correct in the ICEM, and we find $\mathcal{F}^{\psi\psi} \simeq \mathcal{F}^{\psi}$ at the high energy.

The data for the pair J/ψ production cross sections at the energy range 7–13 TeV can be fitted self-consistently with two free parameters $\mathcal{F}^{\psi\psi}$ and σ_{eff}. We have found the best fit with $\mathcal{F}^{\psi\psi} \simeq 0.02$ and $\sigma_{\text{eff}} \simeq 11.0$ mb, when parameter $\mathcal{F}^{\psi}$ is fixed independently in the study of the single J/ψ production. We find the dominant role of the DPS mechanism only in the case of forward pair J/ψ production. At the central region of J/ψ rapidities, both mechanisms contribute approximately equally.

ACKNOWLEDGMENTS

We are grateful to A. Van Hameren for advice on the program KaTie, and M. Nefedov, A. Karpishkov, and A. Shipilova for helpful discussion. The work was supported by the Ministry of Science and Higher Education of the Russian Federation, Project No. FSSS-2020-0014.

[1] J. Badier *et al.* (NA3 Collaboration), Z. Phys. C **20**, 101 (1983).
[2] C. Kourkoumelis *et al.*, Phys. Lett. **91B**, 481 (1980).
[3] A. Adare *et al.* (PHENIX Collaboration), Phys. Rev. Lett. **98**, 232002 (2007).
[4] D. Acosta *et al.* (CDF Collaboration), Phys. Rev. D **71**, 032001 (2005).
[5] R. Aaij *et al.* (LHCb Collaboration), J. High Energy Phys. 11 (2021) 181.
[6] B. Abelev *et al.* (ALICE Collaboration), J. High Energy Phys. 11 (2012) 065.
[7] G. Aad *et al.* (ATLAS Collaboration), Nucl. Phys. **B850**, 387 (2011).
[8] S. Chatrchyan *et al.* (CMS Collaboration), J. High Energy Phys. 02 (2012) 011.
[9] R. Aaij *et al.* (LHCb Collaboration), J. High Energy Phys. 10 (2015) 172; 05 (2017) 063(E).
[10] V. Khachatryan *et al.* (CMS Collaboration), J. High Energy Phys. 09 (2014) 094.
[11] M. Aaboud *et al.* (ATLAS Collaboration), Eur. Phys. J. C **77**, 76 (2017).
[12] R. Aaij *et al.* (LHCb Collaboration), J. High Energy Phys. 06 (2017) 047; 10 (2017) 068(E).
[13] G. T. Bodwin, E. Braaten, and G. P. Lepage, Phys. Rev. D **51**, 1125 (1995); **55**, 5853(E) (1997).
[14] R. Baier and R. Ruckl, Z. Phys. C **19**, 251 (1983).
[15] E. L. Berger and D. L. Jones, Phys. Rev. D **23**, 1521 (1981).
[16] M. Butenschoen, Z.-G. He, and B. A. Kniehl, EPJ Web Conf. **137**, 06009 (2017).
[17] Z.-B. Kang, Y.-Q. Ma, J.-W. Qiu, and G. Sterman, Phys. Rev. D **91**, 014030 (2015).
[18] H. Fritzsch, Phys. Lett. **67B**, 217 (1977).
[19] F. Halzen, Phys. Lett. **69B**, 105 (1977).
[20] Y.-Q. Ma and R. Vogt, Phys. Rev. D **94**, 114029 (2016).
[21] V. Cheung and R. Vogt, Phys. Rev. D **95**, 074021 (2017).
[22] V. Cheung and R. Vogt, Phys. Rev. D **104**, 094026 (2021).
[23] V. Cheung and R. Vogt, Phys. Rev. D **98**, 114029 (2018).
[24] R. Maciuła, A. Szczurek, and A. Cisek, Phys. Rev. D **99**, 054014 (2019).
[25] J. C. Collins and R. K. Ellis, Nucl. Phys. **B360**, 3 (1991).
[26] S. Catani and F. Hautmann, Nucl. Phys. **B427**, 475 (1994).
[27] L. V. Gribov, E. M. Levin, and M. G. Ryskin, Phys. Rep. **100**, 1 (1983).
[28] M. A. Nefedov, V. A. Saleev, and A. V. Shipilova, Phys. Rev. D **87**, 094030 (2013).
[29] A. Karpishkov, M. Nefedov, and V. Saleev, EPJ Web Conf. **158**, 03010 (2017).
[30] M. A. Nefedov and V. A. Saleev, Phys. Rev. D **102**, 114018 (2020).
[31] J. Collins, *Foundations of Perturbative QCD* (Cambridge University Press, Cambridge, England, 2013), Vol. 32, ISBN 978-1-107-64525-7, 978-1-107-64525-7, 978-0-521-85533-4, 978-1-139-09782-6.
[32] L. N. Lipatov, Sov. J. Nucl. Phys. **23**, 338 (1976).
[33] E. A. Kuraev, L. N. Lipatov, and V. S. Fadin, Sov. Phys. JETP **44**, 443 (1976).
[34] E. A. Kuraev, L. N. Lipatov, and V. S. Fadin, Sov. Phys. JETP **45**, 199 (1977).
[35] I. I. Balitsky and L. N. Lipatov, Sov. J. Nucl. Phys. **28**, 822 (1978).
[36] B. A. Kniehl, D. V. Vasin, and V. A. Saleev, Phys. Rev. D **73**, 074022 (2006).
[37] B. A. Kniehl, V. A. Saleev, and D. V. Vasin, Phys. Rev. D **74**, 014024 (2006).
[38] V. A. Saleev, M. A. Nefedov, and A. V. Shipilova, Phys. Rev. D **85**, 074013 (2012).
[39] B. A. Kniehl, M. A. Nefedov, and V. A. Saleev, Phys. Rev. D **94**, 054007 (2016).
[40] A. van Hameren, Comput. Phys. Commun. **224**, 371 (2018).

[41] M. A. Kimber, A. D. Martin, and M. G. Ryskin, Phys. Rev. D **63**, 114027 (2001).
[42] G. Watt, A. D. Martin, and M. G. Ryskin, Eur. Phys. J. C **31**, 73 (2003).
[43] L. N. Lipatov, Nucl. Phys. **B452**, 369 (1995).
[44] L. N. Lipatov and M. I. Vyazovsky, Nucl. Phys. **B597**, 399 (2001).
[45] M. A. Nefedov and V. A. Saleev, Phys. Part. Nucl. **51**, 714 (2020).
[46] M. Nefedov and V. Saleev, Mod. Phys. Lett. A **32**, 1750207 (2017).
[47] M. A. Nefedov, J. High Energy Phys. 08 (2020) 055.
[48] M. A. Nefedov, Nucl. Phys. **B946**, 114715 (2019).
[49] E. N. Antonov, L. N. Lipatov, E. A. Kuraev, and I. O. Cherednikov, Nucl. Phys. **B721**, 111 (2005).
[50] T. Hahn, Comput. Phys. Commun. **140**, 418 (2001).
[51] R. Maciuła, V. A. Saleev, A. V. Shipilova, and A. Szczurek, Phys. Lett. B **758**, 458 (2016).
[52] A. V. Karpishkov, M. A. Nefedov, V. A. Saleev, and A. V. Shipilova, Int. J. Mod. Phys. A **30**, 1550023 (2015).
[53] A. Karpishkov, V. Saleev, and A. Shipilova, Phys. Rev. D **94**, 114012(E) (2016).
[54] V. A. Saleev, M. A. Nefedov, and A. V. Shipilova, Phys. Rev. D **85**, 074013 (2012).
[55] Z.-G. He, B. A. Kniehl, M. A. Nefedov, and V. A. Saleev, Phys. Rev. Lett. **123**, 162002 (2019).
[56] M. G. Ryskin and A. M. Snigirev, Phys. Rev. D **83**, 114047 (2011).
[57] A. van Hameren, P. Kotko, and K. Kutak, J. High Energy Phys. 01 (2013) 078.
[58] A. van Hameren, K. Kutak, and T. Salwa, Phys. Lett. B **727**, 226 (2013).
[59] K. Kutak, R. Maciula, M. Serino, A. Szczurek, and A. van Hameren, J. High Energy Phys. 04 (2016) 175.
[60] J.-P. Lansberg, H.-S. Shao, N. Yamanaka, Y.-J. Zhang, and C. Noûs, Phys. Lett. B **807**, 135559 (2020).